



OPEN ACCESS

EDITED BY Ming Jia,

Dalian University of Technology, China

Aleksandar Ašonja, Business Academy University (Novi Sad), Serbia Abhishek Priyam, SVKM'S NMIMS University, India

*CORRESPONDENCE C. J. Axon, ☑ Colin.Axon@brunel.ac.uk

RECEIVED 12 September 2025 REVISED 07 October 2025 ACCEPTED 13 October 2025 PUBLISHED 19 November 2025

Rrustemi DN, Ganippa LC and Axon CJ (2025) Hydrogen with water addition: an exergy analysis of the internal combustion engine. Front. Mech. Eng. 11:1704197. doi: 10.3389/fmech.2025.1704197

© 2025 Rrustemi, Ganippa and Axon, This is an open-access article distributed under the terms of the Creative Commons Attribution License (CC BY). The use, distribution or reproduction in other forums is permitted, provided the original author(s) and the copyright owner(s) are credited and that the original publication in this journal is cited, in accordance with accepted academic practice. No use, distribution or reproduction is permitted which does not comply with these terms.

Hydrogen with water addition: an exergy analysis of the internal combustion engine

D. N. Rrustemi (1), L. C. Ganippa (1) and C. J. Axon (1) *

Department of Mechanical and Aerospace Engineering, Brunel University of London, London, United Kingdom

The internal combustion engine is likely to be used for on- and off-road vehicles for many years yet, but the push to cease using fossil fuels is strong. Hydrogen is a possible alternative fuel with both advantages and disadvantages, so understanding and quantifying the efficiency losses of burning hydrogen are important. The limits to efficiency and the compromises needed to reduce losses can be investigated using exergy analysis. This analysis of a boosted lean-burn neat hydrogen spark ignition engine investigates exergetic processes under realworld engine operating conditions. Using a two-zone combustion model to study in-cylinder processes, the results suggest exergy transfer to work improves with increasing air dilution by diverting exhaust exergy to reversible work. Injecting water could potentially control emissions through in-cylinder thermo-physical property changes. For an equivalence ratio of 0.45 with 5% water addition, the exergy transfers to heat and work decrease by 12% and 7%, respectively. Conversely, the exergy transfers to combustion-related irreversibility and exhaust rise by 2% and 81%, respectively. However, it was shown that increasing manifold air pressures and compression ratios increases the quantity of exergy directed to work and heat, while reducing exergy expelled to exhaust. This exergy analysis of a hydrogen-fueled spark ignition engine operating under real-world parameters shows the need to optimize water injection as the trade-off between engine performance and emission reductions. Understanding the fundamentals of the thermodynamic mechanisms of work loss may inform engineering improvements to minimize exergy losses and increase efficiency and work output.

combustion, efficiency, entropy, hydrogen, ice, water addition

Highlights

- Exergy divides into work, heat, combustion irreversibility, and exhaust.
- · A fundamental understanding of exergy losses helps engine design and operation
- Injecting water with hydrogen improves combustion and emission performance.
- Water injection increases the exergy expelled by exhaust.

1 Introduction

Hydrogen is a promising alternative fuel with several combustion advantages, such as a higher laminar flame speed, a higher diffusion coefficient, and a wider lean limit than

gasoline (Zaccardi and Pilla, 2019). This means that hydrogen could provide faster reactive combustion, improved fuel and air mixing, and allow the engine to operate under ultra-lean mixtures, thereby increasing thermal efficiency (Verhelst, 2014). However, due to the low volumetric energy of hydrogen/air mixtures, neat hydrogen engines must be boosted to compete with gasoline spark ignition (SI) engines (Berckmüller et al., 2003). Although hydrogen is a carbonfree fuel, the neat hydrogen SI engines can still produce NOx emissions due to the high combustion temperatures (Mortimer et al., 2023). Increasing the intake manifold pressure raises the in-cylinder pressure, which can lead to combustion abnormalities and higher NOx emissions (Gürbüz and Akçay, 2021). Lowering combustion abnormalities and NOx emissions of hydrogen engine could be achieved using exhaust gas recirculation (EGR), lean burn, or water injection (Krishnamoorthi et al., 2019).

As the exhaust of a hydrogen internal combustion engine (ICE) contains high levels of water vapor, it is important to investigate the water addition to the hydrogen-fueled ICE. Injection of water into the port, directly, or into the exhaust manifold of a hydrogen SI engine controls in-cylinder gas temperatures, while intake port injection has been shown to be the most effective in avoiding combustion abnormalities while having minimal impact on efficiency (Boretti, 2024). Water injection cools the chamber mixture because of the higher latent heat of water, which may also reduce NO emissions (Mortimer et al., 2023). Port injection of water to a direct hydrogen SI engine could reduce the NOx emissions by up to 87% with a 2% increase in fuel consumption (Younkins et al., 2015). A reduction of up to 79% at a load of 10 bar and a speed of 2000 rpm, along with a decreased pressure rise rate for port water injection at 5 kg/h in a direct-injected hydrogen SI engine, could improve engine performance and efficiency (Mohamed et al., 2024). Additionally, water injection in a hydrogen SI could extend the knock limit, allowing the use of higher compression ratios, which further improves performance (Mortimer et al., 2023).

The amount and the timing of water injected are relevant as the engine performance decreases by retarding the water injection timing, and due to hydrogen's wide flammability limit, combustion quality is resilient to dilution (Bleechmore and Brewster, 2007). Hydrogen has been used in various dual-fuel and supplementary strategies, such as enrichment in gasoline or natural gas engines, to improve combustion stability and reduce pollutant emissions (Bleechmore and Brewster, 2007). Additionally, the performance of a neat hydrogen-fueled SI engine has been shown to increase with water injection up to 4.05 mg/cycle at an excess air ratio of 1.15 (Xu et al., 2020).

Because the combustion products of hydrogen contain significant water vapor, it is also important to understand the fundamental effects of adding water on combustion. Water addition affects the in-cylinder hydrogen/air mixture via three mechanisms: dilution, thermal diffusion, and chemistry (Duva and Toulson, 2022). These effects are captured by incorporating the empirical correlations for laminar flame speed and specific state properties into a two-zone combustion numerical model of a hydrogen SI engine (Li et al., 2021). Recently developed empirical correlations for the laminar flame speed of hydrogen with water addition can be incorporated into two-zone combustion models that divide the chamber into burned and unburned zones (Rrustemi et al., 2024; Rrustemi et al., 2025a). Hydrogen engines also experience higher heat fluxes than carbon-based fuels; therefore, the Woschni correlation

must be adjusted with appropriate correction factors to accurately predict the heat transfer in hydrogen-fueled SI engines (Krishnanunni et al., 2017).

As the chemical and physical properties of the hydrogen/air mixture vary with water injection, it is beneficial to understand the energy input splits to work, heat, irreversibility, and exhaust of a hydrogen SI engine. Exergy analysis can serve as a method to investigate the fundamental origins of losses, identify efficiency limits, and evaluate the engineering trade-offs necessary to reduce these losses. Exergy is defined as the maximum useful work or available energy, so it can be used to assess the performance of ICEs by identifying and quantifying thermodynamic inefficiencies (Caton, 2000). Exergy destruction is caused by entropy generation initiated by four irreversible processes: chemical reaction, mass diffusion, heat conduction, and viscous dissipation (Nishida et al., 2002). As these processes are complex, it is necessary to understand the relationship between entropy generation and engine operating conditions. Summarizing the exergy analysis of ICEs (Rakopoulos and Giakoumis, 2006) shows that for hydrocarbon fuels, up to a third of input exergy is destroyed by the combustion process (Rakopoulos et al., 2008).

Exergy analysis could reveal fundamental aspects of engine parameter optimization (Abotabik et al., 2020). For example, increasing the temperature of the reactants decreases entropy generation; however, decreasing the equivalence ratio increases combustion-related entropy generation (Knizley et al., 2012). Exergy analysis was applied to various biofuel blends in an SI engine to assess their higher octane suitability and emission reduction potential as cleaner and more sustainable alternatives to conventional gasoline (Mangave et al., 2025). Exergy analysis of SI engines fueled with various biofuels has shown that combustion irreversibility depends on engine operating parameters such as equivalence ratio, EGR, and oxygen concentration, as well as the fuel type. Hydrogen exhibited lower exergy destruction than hydrocarbon biofuels such as ethanol and methanol, reflecting the influence of molecular complexity and oxygen content on combustion efficiency (Caton, 2012).

Comparative exergy analyses of hydrogen, LPG, and gasoline in SI engines show that gasoline achieves a higher exergy transfer to work efficiency than hydrogen due to particular engine operating conditions (Gürbüz and Gülcan, 2025). Exergy analysis was also applied to a neat hydrogen-fueled SI engine at different compression ratios and ignition timings, showing that higher compression ratios improve performance and reduce exergy destruction (Söhret et al., 2019). Moreover, boosting a hydrogen SI engine increases exergy transfer to work due to the rise in in-cylinder pressure, but exergy transfer to heat also increases (Rrustemi et al., 2025b). However, turbocharging improves the use of exhaust exergy (Wang et al., 2019). Operating a hydrogen SI engine at MBT timing increases the thermo-mechanical exergy due to higher in-cylinder pressures, so too the exergy transfer to heat. Retarding the spark timing reduces the exergy expelled at exhaust, while the exergy transfer to combustion-related irreversibility increases due to the drop in incylinder temperatures (Lee et al., 2023), indicating the trade-off between the engine parameters and exergy transfers.

This study investigates the exergy transfers of a hydrogen SI engine with water addition, focusing on manifold air pressure, equivalence ratio, compression ratio, water addition, and emissions.

2 Methodology

2.1 Combustion model

The two-zone combustion model used divides the chamber into two zones: 1) an unburned zone consisting of the fresh charge and 2) a burned zone consisting of the combustion. The main input of the twozone combustion model is the mass fraction burned, which was calculated by introducing an entrainment zone (Ma et al., 2008). As the flame kernel initiates at the spark event, the flame interacts with turbulent motions. Hence, the laminar flame speed experiences wrinkling due to the in-cylinder turbulence. As the flame expands, the entrainment of the unburned gases also increases, causing the flame to advance faster than the rate at which combustion takes place (Conte and Boulouchos, 2005). The combustion itself occurs at the laminar burning rate of the fuel, which is determined by the equivalence ratio, pressure, temperature, and water dilution level (Rrustemi et al., 2024). The entrainment of the unburned gases caused by turbulent interactions occurs at a specific burning time, τ. The entrainment mass fraction of the reactive mixture and the actual mass fraction burned were calculated using Equation 1 and Equation 2, respectively.

$$\frac{dm_{e}}{dt} = \rho_{u}A_{f}\left(S_{l} + u'\right) \tag{1}$$

$$\frac{\mathrm{d}m_{b}}{\mathrm{d}t} = \frac{m_{e} - m_{b}}{\tau_{C}} \tag{2}$$

where m_e is the entrained mass by the flame front, m_b is the burned mass, ρ_u is the unburned mixture density, A_f is the flame front area, S_l is the laminar flame speed (see A2), u' is the in-cylinder turbulence intensity, and τ_C is the characteristic burn-up time. The flame front area A_f was calculated based on the approach proposed by Krebs and Biet (2021). The characteristic burn-up time τ_C was calculated as the ratio of the Taylor micro-scale length L_T to the laminar flame speed, $\tau_C = C_\tau L_T/S_l$. The Taylor micro-scale L_T was calculated as described by Ma et al. (2008). A simple isotropic assumption can be used for turbulence intensity based on the turbulent kinetic energy k, as $u' = \sqrt{\frac{2}{3}k}$. The turbulent kinetic energy k and its dissipation ϵ in Equation 4 were calculated using the established k- ϵ zero-dimensional model in Equation 3 (Krebs and Biet, 2021):

$$\frac{\mathrm{d}k}{\mathrm{d}t} = -\frac{2}{3} \frac{k}{\rho} \frac{\mathrm{d}\rho}{\mathrm{d}t} - \varepsilon \tag{3}$$

$$\varepsilon = \frac{k^{\frac{3}{2}}}{l_*} \tag{4}$$

where the integral turbulent length $l_{\rm I}$ was calculated based on the approach proposed by Hunzinger et al. (2006). The thermodynamics of the hydrogen/air mixture with water addition were calculated using empirical correlations to determine state properties (Heywood, 2018). The NO emissions were calculated using the Zeldovich mechanism (Knop et al., 2008).

2.2 Exergy analysis of the hydrogen ICE

The exergy X of an ICE can be expressed as in Equation 5 (Razmara et al., 2016):

$$X = X_{Chem} + X_{TM} = X_{Work} + X_{Exh} + X_{Irr} + X_{Heat} + X_{others}$$
 (5)

where the X_{Chem} is the chemical exergy and X_{TM} is the thermomechanical exergy. X_{Work} , X_{Exh} , X_{Irr} , and X_{Heat} are exergy transfer to work, heat, irreversibility, and exhaust, respectively. The term X_{others} accounts for exergy transfers that could not be modeled using the current approach, such as exergy destruction from mixing, valve movement, or blow-by gases. The thermal–mechanical and chemical exergy values were calculated by Equation 6 and Equation 7, respectively, while the chemical potential μ was calculated using Equation 8 and Equation 9 (Saxena et al., 2014):

$$X_{TM} = (U - U_{TM}) + P_0(V - V_{TM}) - T_0(S - S_{TM})$$
 (6)

$$X_{\text{Chem}} = \mu_{\text{TM}} - \mu_0 \tag{7}$$

$$\mu_{\rm TM} = h_{\rm TM} - T_0 s_{\rm TM} \tag{8}$$

$$\mu_0 = h_0 - T_0 s_0 \tag{9}$$

where U, V, and S are internal energy, volume, and entropy, respectively. The thermodynamic properties for each species are calculated based on empirical correlations (Heywood, 2018). The subscript TM denotes the restricted dead state, and the subscript 0 corresponds to the dead state. To calculate the physical exergy, a process occurs that changes the temperature and pressure of the system to the restricted dead state TM; however, the system's chemical composition remains unchanged by this process. To calculate the chemical exergy of the system, another process occurs where the chemical composition changes, but the pressure and temperature of the system remain constant ($P_{\rm TM}=P_0=1$ bar and $T_{\rm TM}=T_0=298.15$ K). Note that the system boundary for the exergy analysis was defined by the combustion chamber walls and the piston head.

The exergy was split into four contributors: work, heat, irreversibility, and exhaust. The exergy transfer to indicated work is given by Equation 10 (Caton, 2012):

$$\frac{dX_{\text{Work}}}{d\theta} = (P - P_0) \frac{dV}{d\theta}$$
 (10)

where P is the instantaneous in-cylinder pressure obtained from the two-zone hydrogen combustion model, P_0 is the pressure at the dead state, and V is the volume of the cylinder. The exergy transfer to heat caused by the difference between the in-cylinder mixture and chamber wall is given by Equation 11 (Lee et al., 2023):

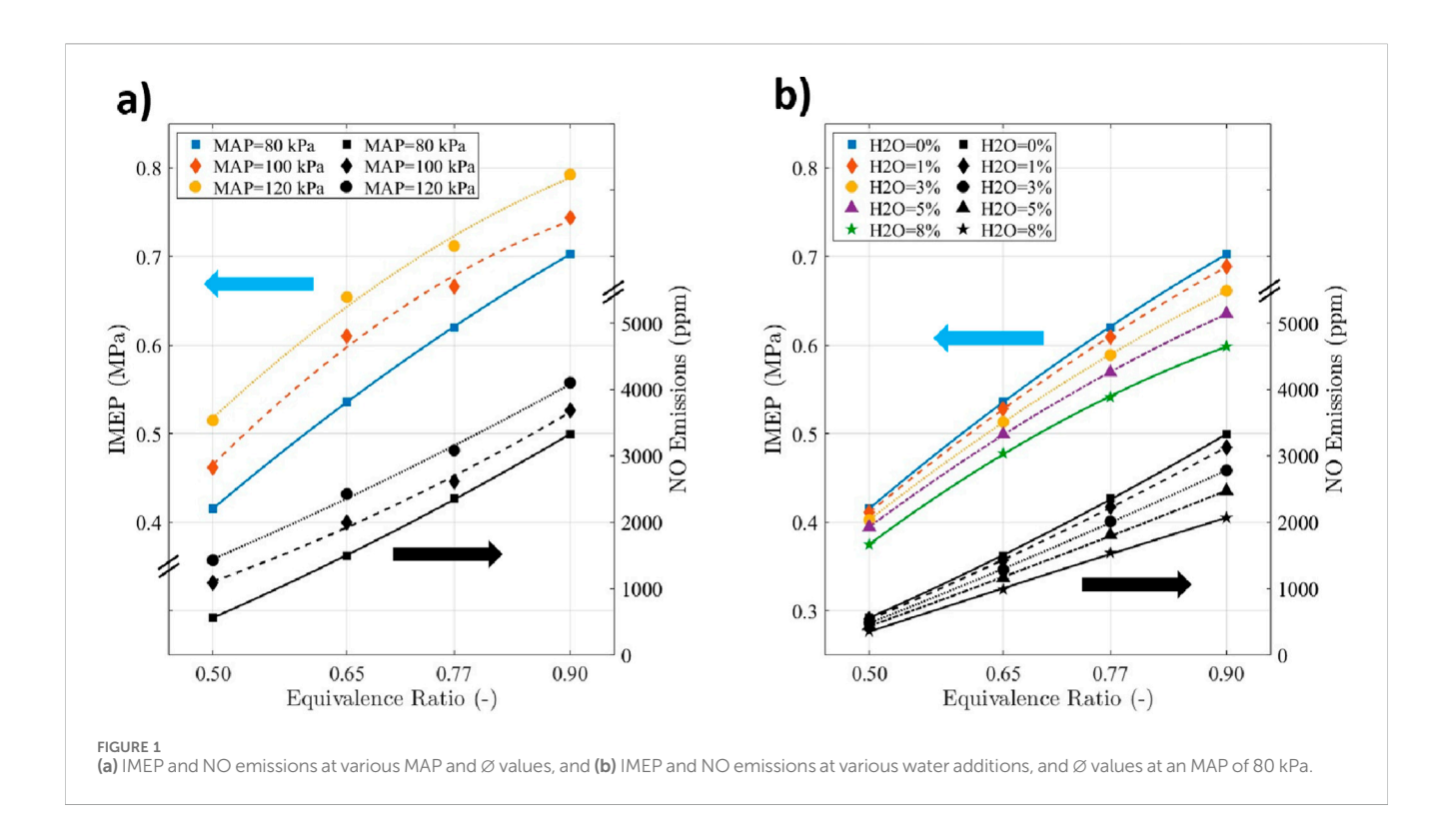
$$\frac{dX_{Heat}}{d\theta} = -\left(1 - \frac{T_0}{T}\right) \frac{dQ_{ht}}{d\theta}$$
 (11)

where T_0 and T are the initial and in-cylinder temperatures, respectively. The convective heat loss Q_{ht} is modeled using the Woschni correlation (Woschni, 1967). However, to accurately reflect the heat losses associated with hydrogen combustion, the heat transfer coefficient from the standard Woschni correlation was multiplied by a factor of 2.2 (Krishnanunni et al., 2017).

The chemical exergy of hydrogen was calculated using Equation 12 (Pozzato et al., 2022):

$$X_{CH} = (U_{TM} + P_0 V_{TM} - T_0 S_{TM}) - \sum_{i} \sum_{j} \mu_{i,0} \left(\frac{v_{ij}}{v_j}\right) N_j$$
 (12)

where the chemical exergy X_{CH} is the chemical potential at the restricted dead state, as well as the chemical potential of the environmental species j, which are formed from the species i originally present in the system at



the environmental dead state. The environment is considered to consist of four main species, with all remaining components grouped into a single category. The volume fractions of these species are: $20.35\% O_2$, $75.67\% N_2$, $0.03\% CO_2$, $3.03\% H_2O$, and 0.92% for other components (Rakopoulos and Giakoumis, 2006).

The exergy destroyed by combustion-related irreversibility was calculated as a function of the reaction rate and the difference between the chemical potential of the reactants and products. The combustion irreversibility is given by Equation 13 (Rakopoulos and Giakoumis, 2006):

$$\frac{dX_{Comb}}{d\theta} = -T_0 \frac{dS_{Gen}}{d\theta} = -\frac{T_0}{T} \sum_i \mu_{i,0} dm_i \eqno(13)$$

where the chemical potential μ_i is set to be X_{Chem} for the fuel and to be the Gibbs free energy G_i for other gases. Finally, the exergy expelled by the exhaust gases is defined as the thermo-mechanical exergy available at exhaust valve opening (EVO) in Equation 14 (Razmara et al., 2016):

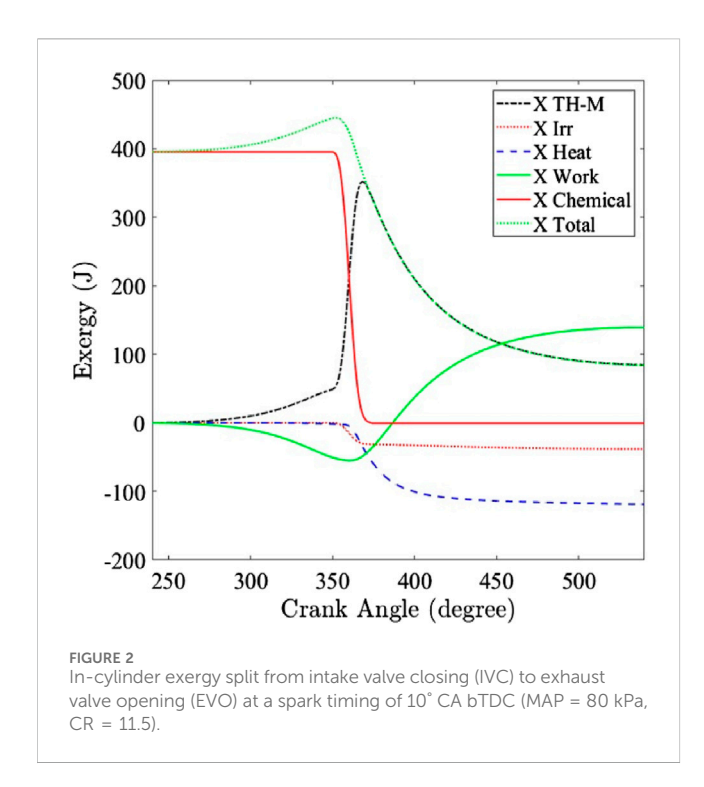
$$X_{\text{exh}} = X_{\theta = \text{EVO}} \tag{14}$$

3 Results and discussion

3.1 Engine performance

Figure 1a shows the indicated mean effective pressure (IMEP) of the boosted hydrogen SI engine at various equivalence ratios under MBT timing. It can be seen that the IMEP increases monotonically at all presented equivalence ratios with increasing manifold air pressure (MAP) values. At an equivalence ratio of 0.9, the IMEP increased by 6% and 13% when the MAP was increased from 80 kPa to 100 kPa and 120 kPa, respectively. The IMEP increase with boosting could be due to the increase in the amount of hydrogen at higher MAP values (Berckmüller et al., 2003). Additionally, the IMEP decreases with decreasing equivalence ratios because of the reduced fuel mass in leaner mixtures. Under naturally aspirated conditions (MAP = 80 kPa), the IMEP decreased by 12%, 24%, and 41% when equivalence ratios were reduced from 0.9 to 0.77, 0.65, and 0.5, respectively.

The benefit of increasing MAP is countered by the rise in NO emissions. Under an equivalence ratio of 0.9, the NO emissions increase by 11%, and 23% when the MAP increases from 80 kPa to 100 kPa and 120 kPa, respectively. This was because of the increase in in-cylinder pressure due to higher charge density for higher MAP values, which increases the turbulence intensity, consequently decreasing the combustion duration captured by Equation 1. Thus, it increases the in-cylinder temperature, which could be mitigated by decreasing the equivalence ratio. Under naturally aspirated conditions (MAP = 80 kPa), the NO emissions were reduced by 30%, 55% and 83% when the equivalence ratio was reduced from 0.9 to 0.77, 0.65, and 0.5, respectively; as was the load (Figure 1a). This could be due to the reduction in the in-cylinder temperature for leaner hydrogen-with-air mixtures. At an MAP of 80 kPa and an Ø of 0.9, the NO emissions decreased by 6%, 16%, 26%, and 38% for 1%, 3%, 5%, and 8% water additions, respectively. This reduction was due to the lower in-cylinder temperatures as water decreases the combustion flame speed and increases the heat capacity. However, the IMEP was reduced by 6% and 38% for 1% and 8% water additions, respectively (Figure 1b). The amount of water injected can be optimized to balance the trade-off between IMEP and NO emissions. For instance, when 1% water was added at an equivalence ratio of 0.9 with a boost of 40 kPa, NO emissions decreased by 5%.

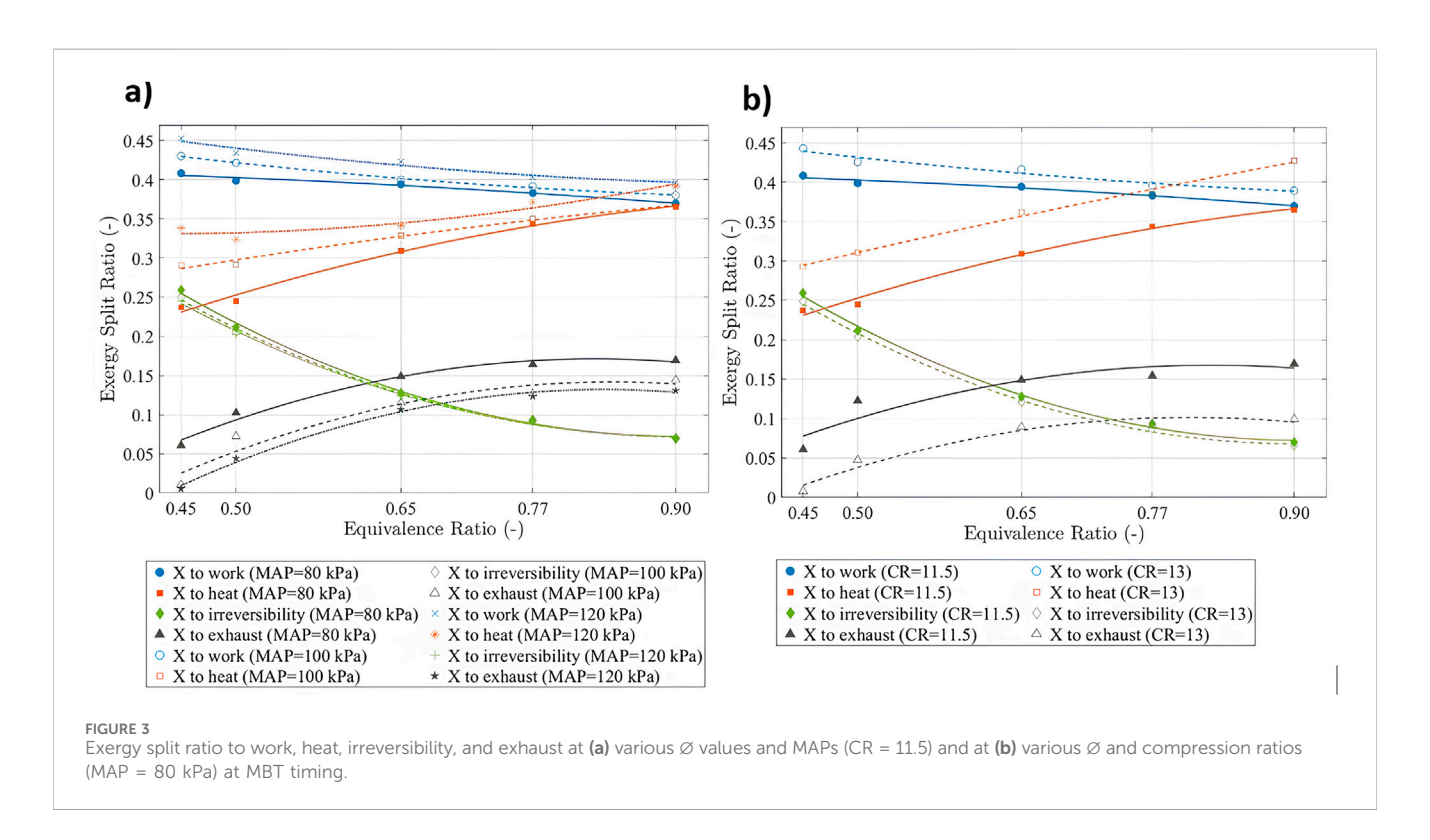


3.2 Exergy analysis

Because hydrogen's high reactivity and simple molecular structure differ greatly from hydrocarbon fuels, this section analyzes the exergy transfer to work, heat, irreversibility, and exhaust of a hydrogen SI engine at various water additions, manifold air pressures, equivalence ratios, and compression

ratios. In Figure 2, the instantaneous exergy contributors of work, heat, and combustion irreversibility are presented as a function of crank angle from intake valve closing (IVC) to exhaust valve opening (EVO). During compression, the thermomechanical exergy increases as the in-cylinder pressure and temperature rise, whereas the exergy attributed to heat transfer remains insignificant. With the start of combustion at 10° crank angle (degrees) before top dead center (CA bTDC), the chemical exergy decreases significantly due to the fuel being burned, while the thermo-mechanical exergy increases as the chemical exergy is converted to mechanical exergy during combustion. Similarly, the exergy transfer to heat increases as the in-cylinder temperature rises, continuing through the expansion process. At the end of combustion, the total in-cylinder exergy decreases due to exergy transfers to work, heat, and combustion-related irreversibility. The remaining total in-cylinder exergy at EVO is defined as the exergy available at exhaust, as the in-cylinder pressure and temperature are still higher than those of the dead state.

Figure 3 shows the exergy split ratio defined as the proportion of the exergy transfer to work, heat, irreversibility, and exhaust, relative to the corresponding intake exergy. It can be seen from Figure 3 that in all presented cases, the largest exergy contributor is the transfer to reversible work. As the mixture becomes leaner, the exergy transfer to work increases. Under naturally aspirated conditions (MAP = 80 kPa), the exergy transfer to work increased by 4%, 7%, 8%, and 10% when the Ø decreased from 0.9 to 0.77, 0.65, 0.5, and 0.45, respectively. This increase is due to the greater amount of work extracted from leaner mixtures due to the increased specific heat ratio. As a result, less exergy remains to be expelled through the exhaust. Exhaust exergy represents the available in-cylinder exergy at EVO, and once the mixture interacts with the environment, the exergy is destroyed. Additionally, in leaner mixtures, exhaust



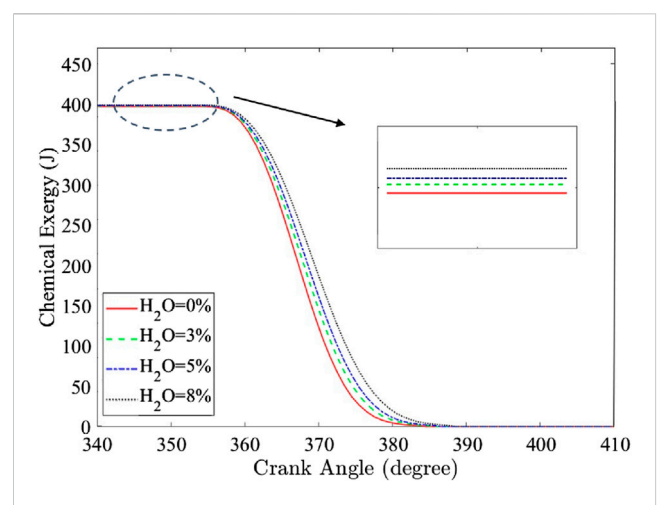
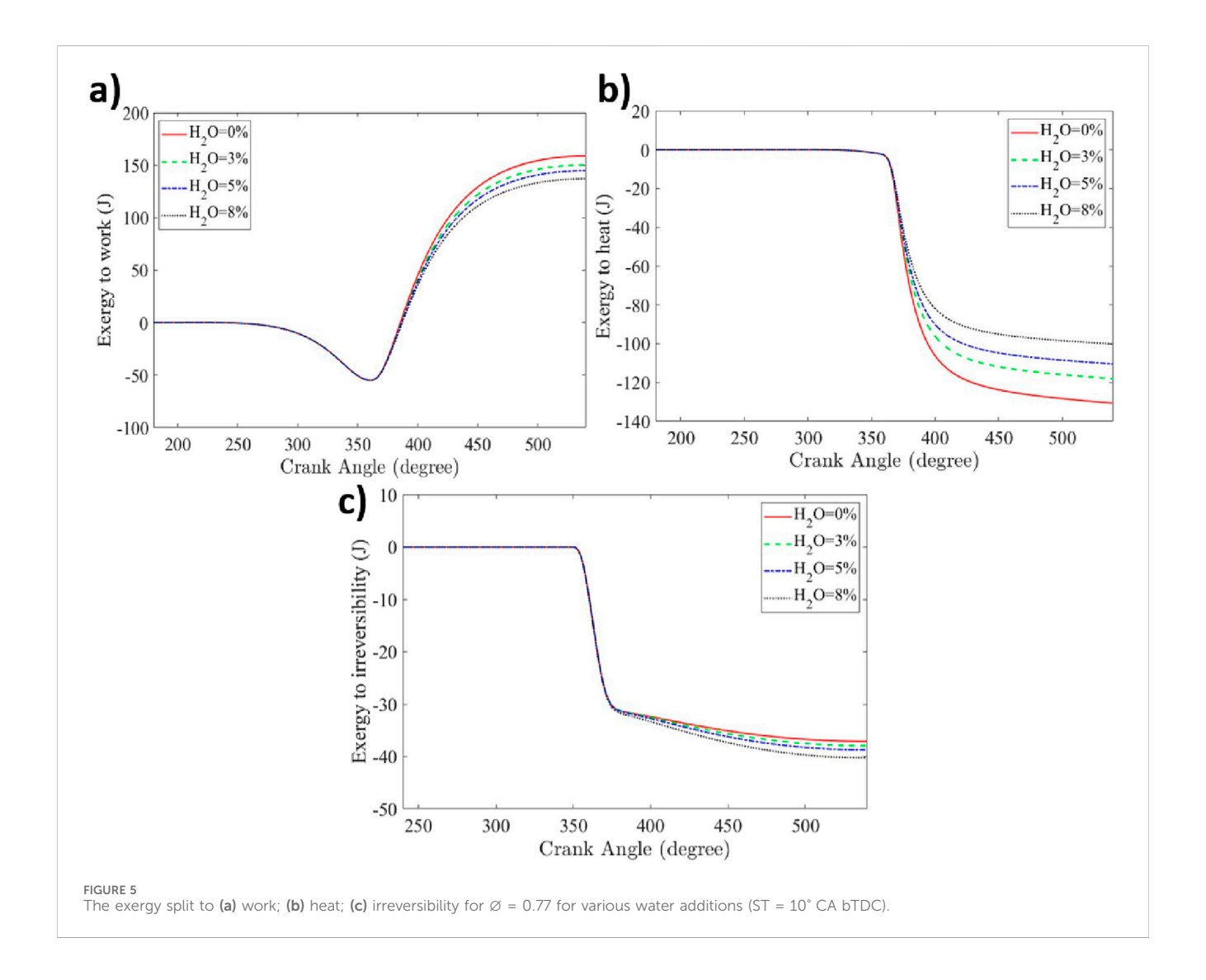


FIGURE 4 Hydrogen/air chemical exergy at different water additions for the naturally aspirated condition under an \varnothing of 0.77 (ST = 5° CA bTDC, MAP = 80 kPa, N = 2000 rpm). The inset demonstrates that water increases the chemical exergy because its chemical potential is greater than that of air.

enthalpy is converted into useful work. Under naturally aspirated conditions (MAP = 80 kPa), the exergy transfer to the exhaust decreases by 9%, 12%, 28%, and 64% when the \varnothing decreases from 0.9 to 0.77, 0.65, 0.5, and 0.45, respectively.

In contrast, it can be seen from Figure 3a that the exergy transfer to heat decreases for leaner mixtures due to a drop in in-cylinder energy content (less fuel), which in turn lowers the in-cylinder temperature, reducing the temperature difference between the mixture and the chamber wall. Under naturally aspirated conditions (MAP = 80 kPa), the exergy transfer to heat decreased by 6%, 15%, 32%, and 35% when the Ø decreased from 0.9 to 0.77, 0.65, 0.5, and 0.45, respectively. A portion of the exergy is destroyed by combustion-related irreversibility. The exergy transfer to combustion-related irreversibility increased by 3%, 82%, 201%, and 269% when the \varnothing decreased from 0.9 to 0.77, 0.65, 0.5, and 0.45, respectively, for an MAP of 80 kPa. Under the naturally aspirated condition, at an Ø of 0.45, the exergy transfer to combustion irreversibility was 26%, limiting the maximum possible efficiency to 74% for this case. The exergy transfer to combustion irreversibility increases due to the greater entropy difference between reactants and products for leaner mixtures (less hydrogen).



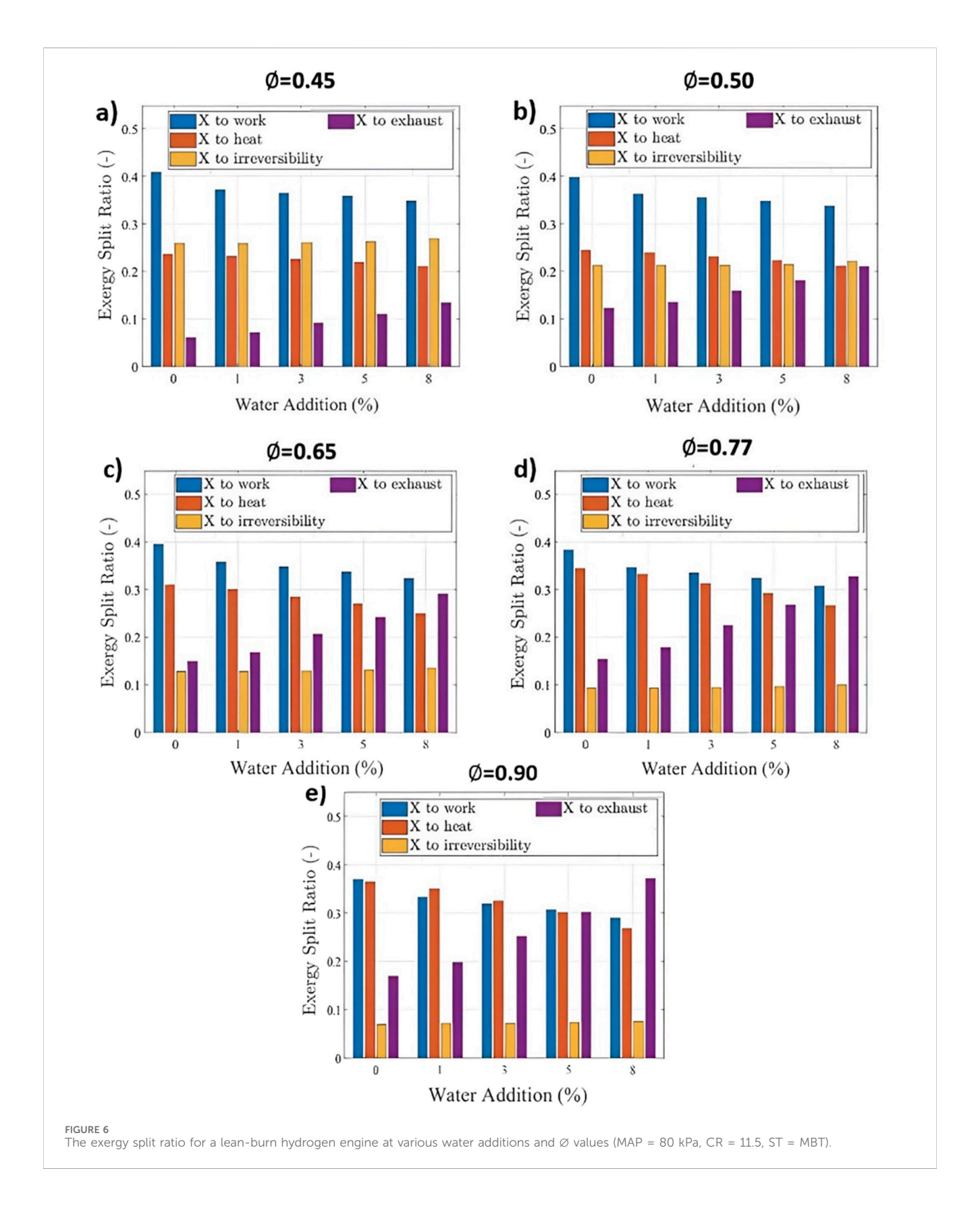


Figure 3a also shows that increasing MAP values increases the exergy transfer to work and heat. Under an \varnothing of 0.9, the exergy transfer to work increases by 3% and 7% when the MAP increases from 80 kPa to 100 kPa and 120 kPa, respectively. Similarly, at an \varnothing

of 0.9, the exergy transfer to heat increased by 4% and 7% when the MAP increased from 80 kPa to 100 kPa and 120 kPa, respectively. This is due to the increase in the charge density, increasing incylinder pressure and temperature, and consequently increasing the

difference between in-cylinder charge and wall temperature. In contrast, the exergy expelled by the exhaust decreases as the MAP increases due to exergy being diverted into work and heat. The exergy transfer to the exhaust decreases slightly due to the increased in-cylinder temperature. Similarly, increasing the compression ratio (Figure 3b) increases the exergy transfer to work and heat and reduces the exergy transfer to exhaust. By increasing the compression ratio from 11.5 to 13, the exergy transfer to work increased by 9%, 7%, 6%, 4%, and 3% for an Ø of 0.45, 0.5, 0.65, 0.77, and 0.9, respectively. This may be due to the increase in in-cylinder pressure and temperature during the compression process at higher compression ratios, which could increase the flame speed and subsequently reduce the combustion duration (Salvi and Subramanian, 2022). The peak exergy transfer to work of 44% occurred for an \emptyset of 0.45 at a compression ratio of 13. The exergy transfer to combustion irreversibility did not vary significantly with increasing compression ratio. For an \emptyset of 0.9, the exergy transfer to combustion irreversibility reached a plateau at 7%, even though the in-cylinder energy state increased with increasing compression ratio. However, increasing the compression ratio was effective in reducing the exergy expelled by the exhaust. By increasing the compression ratio from 11.5 to 13, the exergy transfer to the exhaust was reduced by 88%, 41%, and 37% for \varnothing values of 0.45, 0.5, 0.65, 0.77, and 0.9, respectively.

3.3 Water effect on exergy split to work, heat, irreversibility, and exhaust

Water injection reduces NO emissions, but the effect on the exergy split into work, heat, irreversibility, and exhaust must also be understood. The chemical exergy decreases proportionally to the mass fraction burned and decreases progressively as combustion occurs. The reducing slope of chemical exergy during combustion of Figure 4 shows that adding water to hydrogen combustion increases the combustion duration due to the decrease in laminar flame speed (LFS) and the increase in the heat capacity of the in-cylinder mixture due to the slower combustion process. The exergy transfer to work and heat shown in Figures 5a,b, respectively, decreases with higher water additions, primarily due to the high specific heat capacity of water. The exergy to heat at EVO was reduced by 2%, 15%, and 23% for 3%, 5%, and 8% water additions, respectively. Even though the heat transfer decreased, it did not divert the remaining exergy to work. Additionally, the exergy transfer to work at EVO decreases by 5%, 9%, and 14% for 3%, 5%, and 8% water addition, respectively. In contrast, as shown in Figure 5c, the exergy transfer to combustionrelated irreversibility increases with water addition, with increases of 2%, 4%, and 9% at EVO for 3%, 5%, and 8% water additions, respectively. This could be due to the increase in entropy generation due to the rise of product entropy and reduction of the in-cylinder temperature with water addition (Rrustemi et al., 2025a).

Figure 6 shows that as water addition increases, the exergy transfer to work decreases due to the reduced in-cylinder pressure. For an \varnothing of 0.45 (Figure 6a), the exergy transfer to work decreases by 9%, 11%, 12%, and 14% with 1%, 3%, 5%, and 8% water additions, respectively. Similarly, as water addition increases, exergy transfer to heat decreases due to the drop in in-cylinder temperature, with reductions of 2%, 5%, 7%, and 11% for the same levels of water

addition. Conversely, exergy destroyed by combustion-related irreversibility increases with water addition. This is attributed to the rise in product entropy and the decrease in in-cylinder temperature. Exergy loss to irreversibility increases by 1%, 2%, and 4% with 3%, 5%, and 8% water additions, respectively. As exergy transfers to work and heat decrease with water addition due to the higher specific heat capacity of water, the remaining exergy expelled through the exhaust increases. This agrees with the second law of thermodynamics, which states that a steady-state system must reject the remaining generated entropy. For an \varnothing of 0.5, the exergy expelled by the exhaust gases increases by 18%, 51%, 81%, and 121% with 1%, 3%, 5%, and 8% water additions, respectively. Without any further mechanical improvements, the heat reduction by water addition in a hydrogen SI engine does not increase the exergy transfer to work; rather, it expels exergy through the exhaust. This suggests potential for utilizing exergy in the exhaust of water-diluted hydrogen SI engines.

4 Conclusion

A two-zone hydrogen combustion was used to identify the exergy transfer to work, heat, irreversibility, and exhaust of a boosted lean-burn hydrogen SI engine with water addition. Increasing manifold air pressure boosts the performance of the hydrogen SI engine but also increases NO emissions. NO emissions were mitigated by reducing the equivalence ratio and by water injection. Water injection effectively and significantly reduced NO emissions, but it came at the cost of reduced IMEP, requiring optimization between performance and emissions. For an equivalence ratio of 0.9 under naturally aspirated conditions with 1% water addition, NO emissions decreased by 6% with a 2% IMEP decrease. The analysis was achieved using the second law of thermodynamics to identify and quantify the exergy transfer to work, heat, irreversibility, and exhaust at various MAPs, equivalence ratios, compression ratios, and water additions. The exergy transfer to work increases with reducing equivalence ratio, as the exhaust enthalpy is diverted into useful work. However, the exergy split to combustionrelated irreversibility also increases due to the reduced amount of hydrogen fuel at lower equivalence ratios. For naturally aspirated conditions at an equivalence ratio of 0.45, approximately 26% of the input exergy was transferred to combustion irreversibility, limiting the maximum possible efficiency to 74%. Additionally, increasing the MAP and compression ratio was shown to increase exergy transfer to heat and work, leaving less exergy to be expelled by the exhaust. The exergy transfer to combustion irreversibility was not significantly affected by the MAP or compression ratio. Adding water to the hydrogen SI engine decreased the exergy transfer to work and heat due to slower combustion, which was caused by the increased heat capacity of the hydrogen/air mixture with water addition. In contrast, exergy transfer to irreversibility increased because of lower in-cylinder temperatures. The remaining exergy was expelled through the exhaust, and this increased with higher water additions. For an equivalence ratio of 0.45 with 5% water addition, the exergy transfer to heat and work decreases by 12% and 7%, respectively. In contrast, the exergy transfer to combustion-related irreversibility and exhaust increases by 2% and 81%, respectively.

This study considered the exergy transfer to work, heat, combustion irreversibility, and exhaust to indicate their relative

importance, but it could not capture the spatial effects of water addition on in-cylinder mixture formation, which would require more advanced multidimensional modeling. The aim was to understand how to manage resources to maximize work output while minimizing energy input and emissions. A hydrogen SI engine requires an increase in IMEP to compete with gasoline engines, which can be achieved by increasing the MAP or the compression ratio. Hence, the need to understand the exergy split into work, heat, irreversibility, and exhaust. Finally, it can be highlighted that water addition reduces NO emissions in a hydrogen-fueled SI engine and has further potential to optimize the exhaust exergy. Although the combustion model and exergy analysis in this study were developed for hydrogen, the methodology is also applicable to the optimization of other alternative-fueled SI engines. Exergy analysis of different fuels could reveal opportunities to improve engine thermal efficiency through the application of second-law-based engine control strategies.

Data availability statement

The raw data supporting the conclusions of this article will be made available by the authors, without undue reservation.

Author contributions

DR: Data curation, Formal Analysis, Investigation, Methodology, Software, Validation, Visualization, Writing – original draft. LG: Conceptualization, Methodology, Writing – review and editing. CA: Conceptualization, Methodology, Supervision, Writing – review and editing.

References

Abotabik, M., Meyer, R., and Proctor, C. (2020). "Exergy based optimal controller design of a spark-ignition internal combustion engine,". Technical Paper 2020-01-0250. Detroit, MI: SAE International. doi:10.4271/2020-01-0250

Berckmüller, M., Rottengruber, H., Eder, A., Brehm, N., Elsässer, G., Müller-Alander, G., et al. (2003). "Potentials of a charged SI-Hydrogen engine,". Technical Paper 2023-01–3210. Pittsburgh, PA: SAE International. doi:10.4271/2003-01-3210

Bleechmore, C., and Brewster, S. (2007). Dilution strategies for load and NOx management in a hydrogen fuelled direct injection engine, Rosemont, IL: SAE International, Technical Paper 2007-01-4097. doi:10.4271/2007-01-4097

Boretti, A. (2024). Water injection strategies to control gas temperatures in hydrogen–air internal combustion engines. *J. Braz Soc. Mech. Sci. Eng.* 46, 54. doi:10.1007/s40430-023-04623-x

Caton, J. A. (2000). A review of investigations using the second law of thermodynamics to study internal-combustion engines, Detroit, MI: SAE International, Technical Paper 2000-01–1081. doi:10.4271/2000-01-1081

Caton, J. A. (2012). Exergy destruction during the combustion process as functions of operating and design parameters for a spark-ignition engine. *Int. J. Energy Res.* 36, 368–384. doi:10.1002/er.1807

Conte, E., and Boulouchos, K. (2005). A quasi-dimensional model for estimating the influence of hydrogen-rich gas addition on turbulent flame speed and flame front propagation in IC-SI engines. *J. ENGINES* 1. doi:10.4271/2005-01-0232

Duva, B. C., and Toulson, E. (2022). Unstretched unburned flame speed and burned gas Markstein length of diluted hydrogen/air mixtures. *Int. J. Hydrog. Energy* 47, 9030–9044. doi:10.1016/j.ijhydene.2021.12.217

Gürbüz, H., and Akçay, İ. H. (2021). Evaluating the effects of boosting intake-air pressure on the performance and environmental-economic indicators in a hydrogenfueled SI engine. *Int. J. Hydrog. Energy* 46, 28801–28810. doi:10.1016/j.ijhydene.2021. 06.099

Funding

The author(s) declare that no financial support was received for the research and/or publication of this article.

Conflict of interest

The authors declare that the research was conducted in the absence of any commercial or financial relationships that could be construed as a potential conflict of interest.

Generative AI statement

The author(s) declare that no Generative AI was used in the creation of this manuscript.

Any alternative text (alt text) provided alongside figures in this article has been generated by Frontiers with the support of artificial intelligence and reasonable efforts have been made to ensure accuracy, including review by the authors wherever possible. If you identify any issues, please contact us.

Publisher's note

All claims expressed in this article are solely those of the authors and do not necessarily represent those of their affiliated organizations, or those of the publisher, the editors and the reviewers. Any product that may be evaluated in this article, or claim that may be made by its manufacturer, is not guaranteed or endorsed by the publisher.

Gürbüz, H., and Gülcan, H. E. (2025). Energy, exergy, and exergoeconomic analysis of the use of hydrogen, LPG, and gasoline in an air-cooled SI engine running at stoichiometric conditions. *Int. J. Hydrog. Energy* 138, 1170–1179. doi:10.1016/j. ijhydene.2025.03.226

Heywood, J. B. (2018). *Internal combustion engine fundamentals*. New York: Mcgraw-Hill Education.

Hunzinger, N., Rothe, M., Spicher, U., Gegg, T., Rieber, M., Klimmek, A., et al. (2006). "Quasi-dimensional combustion simulation of a Two- stroke engine. Technical Paper 2006-32–0062. San Antonio, TX: SAE International, 2006. doi:10.4271/2006-32-0062

Knizley, A. A., Srinivasan, K. K., Krishnan, S. R., and Ciatti, S. A. (2012). Fuel and diluent effects on entropy generation in a constant internal energy-volume (uv) combustion process. *Energy* 43, 315–328. doi:10.1016/j.energy.2012.04.024

Knop, V., Benkenida, A., Jay, S., and Colin, O. (2008). Modelling of combustion and nitrogen oxide formation in hydrogen-fuelled internal combustion engines within a 3D CFD code. *Int. J. Hydrog. Energy* 33, 5083–5097. doi:10.1016/j.ijhydene.2008.06.027

Krebs, S., and Biet, C. (2021). Predictive model of a premixed, lean hydrogen combustion for internal combustion engines. *Transp. Eng.* 5, 100086. doi:10.1016/j.treng.2021.100086

Krishnamoorthi, M., Malayalamurthi, R., He, Z., and Kandasamy, S. (2019). A review on low temperature combustion engines: performance, combustion and emission characteristics. *Renew. Sustain Energy Rev.* 116, 109404. doi:10.1016/j.rser.2019.109404

Krishnanunni, J., Bhatia, D., and Das, L. M. (2017). Experimental and modelling investigations on the performance and emission characteristics of a single cylinder hydrogen engine. *Int. J. Hydrog. Energy* 42, 29574–29584. doi:10.1016/j.ijhydene.2017. 10.018

Lee, S., Kim, Y., Lee, J., Kim, K., Lee, S., Min, K., et al. (2023). Energy and exergy analyses of hydrogen-fueled spark ignition engine with various air excess ratios and ignition timings. *Fuel* 349, 128588. doi:10.1016/j.fuel.2023.128588

Li, R. C., Zhu, G. G., and Men, Y. (2021). A two-zone reaction-based combustion model for a spark-ignition engine. *Int. J. Engine Res.* 22, 109–124. doi:10.1177/1468087419841746

Ma, F., Liu, H., Wang, Y., Wang, J., Ding, S., and Zhao, S. (2008). A quasi-dimensional combustion model for SI engines fuelled by hydrogen enriched compressed natural gas. *Energy Procedia* 1, 1633. doi:10.4271/2008-01-1633

Mangave, P. P., Pawar, N. D., Patil, R. S., Patil, V. V., and Kumar, S. (2025). Energy and exergy analysis of a SI engine fueled with anisole and isobutyl acetate with superpremium gasoline. *Proc. Inst. Mech. Eng. Part C J. Mech. Eng. Sci.* 239, 2202–2216. doi:10.1177/09544062241296924

Mohamed, M., Biswal, A., Wang, X., Zhao, H., Harington, A., Hall, J., et al. (2024). Exploring the benefits of hydrogen-water injection technology in internal combustion engines: a rigorous experimental study. *Int. J. Engine Res.* 26, 724–740. doi:10.1177/ 14680874241288624

Mortimer, J., Poursadegh, F., Brear, M., Yoannidis, S., Lacey, J., and Yang, Y. (2023). Extending the knock limits of hydrogen DI ICE using water injection. *Fuel* 335, 126652. doi:10.1016/j.fuel.2022.126652

Nishida, K., Takagi, T., and Kinoshita, S. (2002). Analysis of entropy generation and exergy loss during combustion. *Proc. Combust. Inst.* 29, 869–874. doi:10.1016/S1540-7489(02)80111-0

Pozzato, G., Rizzo, D. M., and Onori, S. (2022). Mean-value exergy modeling of internal combustion engines: characterization of feasible operating regions. *J. Dyn. Syst. Meas. Control* 144, 061009. doi:10.1115/1.4053945

Rakopoulos, C., and Giakoumis, E. (2006). Second-law analyses applied to internal combustion engines operation. *Prog. Energy Combust. Sci.* 32, 2–47. doi:10.1016/j.pecs. 2005.10.001

Rakopoulos, C. D., Michos, C. N., and Giakoumis, E. G. (2008). Availability analysis of a syngas fueled spark ignition engine using a multi-zone combustion model. *Energy* 33, 1378–1398. doi:10.1016/j.energy.2008.05.007

Razmara, M., Bidarvatan, M., Shahbakhti, M., and Robinett, R. D. (2016). Optimal exergy-based control of internal combustion engines. *Appl. Energy* 183, 1389–1403. doi:10.1016/j.apenergy.2016.09.058

Rrustemi, D. N., Ganippa, L. C., Megaritis, T., and Axon, C. J. (2024). New laminar flame speed correlation for lean mixtures of hydrogen combustion with water addition under high pressure conditions. *Int. J. Hydrog. Energy* 63, 609–617. doi:10.1016/j.ijhydene.2024.03.177

Rrustemi, D. N., Ganippa, L. C., Megaritis, T., and Axon, C. J. (2025a). Predicting hydrogen engine performance with water addition using a two-zone thermodynamic model. *Fuel* 386, 134137. doi:10.1016/j.fuel.2024.134137

Rrustemi, D. N., Ganippa, L. C., and Axon, C. J. (2025b). Exergy analysis of the lean-burn hydrogen-fuelled engine. *Energy* 314, 134110. doi:10.1016/j.energy. 2024.134110

Salvi, B. L., and Subramanian, K. A. (2022). A novel approach for experimental study and numerical modeling of combustion characteristics of a hydrogen fuelled spark ignition engine. *Sustain Energy Technol. Assess.* 51, 101972. doi:10.1016/j.seta.2022.101972

Saxena, S., Shah, N., Bedoya, I., and Phadke, A. (2014). Understanding optimal engine operating strategies for gasoline-fueled HCCI engines using crank-angle resolved exergy analysis. *Appl. Energy* 114, 155–163. doi:10.1016/j.apenergy.2013. 09 056

Şöhret, Y., Gürbüz, H., and Akçay, İ. H. (2019). Energy and exergy analyses of a hydrogen fueled SI engine: effect of ignition timing and compression ratio. *Energy* 175, 410–422. doi:10.1016/j.energy.2019.03.091

Verhelst, S. (2014). Recent progress in the use of hydrogen as a fuel for internal combustion engines. *Int. J. Hydrog. Energy* 39, 1071–1085. doi:10.1016/j.ijhydene.2013. 10.102

Wang, X., Sun, B., and Luo, Q. (2019). Energy and exergy analysis of a turbocharged hydrogen internal combustion engine. *Int. J. Hydrog. Energy* 44, 5551–5563. doi:10. 1016/j.ijhydene.2018.10.047

Woschni, G. (1967). A universally applicable equation for the instantaneous heat transfer coefficient in the internal combustion engine. Technical Paper 1967-67–0931. SAE International. 1. 670931. doi:10.4271/670931

Xu, P., Ji, C., Wang, S., Cong, X., Ma, Z., Tang, C., et al. (2020). Effects of direct water injection on engine performance in engine fueled with hydrogen at varied excess air ratios and spark timing. *Fuel* 269, 117209. doi:10.1016/j.fuel.2020.117209

Younkins, M., Wooldridge, M. S., and Boyer, B. A. (2015). Port injection of water into a DI hydrogen engine. Technical Paper 2015-01–0861. Detroit, MI: SAE International. doi:10.4271/2015-01-0861

Zaccardi, J.-M., and Pilla, G. (2019). Hydrogen as a combustion enhancer for highly efficient ultra-lean spark-ignition engines, Kyoto, JP: SAE International, Technical Paper 2019-01–2258. doi:10.4271/2019-01-2258

Nomenclature

Symbols

specific heat (J/kgK)

dissipation

Stefan–Boltzmann constant (5.67 $\times~10^{-8}~W/m^2K^4)$

specific enthalpy (J/kg) h

species index

environmental species index

kinetic energy (m^2/s^2)

length (m)

mass (kg) m

chemical potential (J/mol)

number of moles (mol) n

pressure (Pa)

Ø equivalence ratio

heat (J) Q

universal gas constant (8.314 J/mol K) R

density (kg/m³)

entropy (J/K) S

Laminar flame speed (m/s) S_L

temperature (K)

eddy burn time

crank angle (degrees) θ

specific internal energy (J)

turbulent intensity (m/s) u'

volume (m³)

stoichiometric coefficient

exergy (J) Х

Acronyms

bTDC before top dead centre

CA crank angle

CR compression ratio

EGR exhaust gas recirculation

EVO exhaust valve opening (crank angle)

 H_2O water vapor

ICE internal combustion engine

IMEP indicated mean effective pressure (Pa)

ITE indicated thermal efficiency (%)

IVC intake valve closing (crank angle) manifold air pressure (Pa)

MBT maximum brake torque

NO nitric oxide

MAP

NOx oxides of nitrogen

Subscripts

dead state

burn

chem chemical

exhaust Exh

entrained

htheat transfer

irreversibility Irr

TMthermo-mechanical

TMrestricted dead state

Work work